Rainfall Field Reconstruction by Opportunistic Use of the Rain-Induced Attenuation on Microwave Satellite Signals: The July 2021 Extreme Rain Event in Germany as a Case Study

Fabiola Sapienza
Dept. Information Engineering
University of Pisa
Pisa, Italy
fabiola.sapienza@ing.unipi.it

Giacomo Bacci
Dept. Information Engineering
University of Pisa
Pisa, Italy
giacomo.bacci@unipi.it

Filippo Giannetti
Dept. Information Engineering
University of Pisa
Pisa, Italy
filippo.giannetti@unipi.it

Michele Gammone *MBI srl*
Pisa, Italy
mgammone@mbigroup.it

Vincenzo Lottici
Dept. Information Engineering
University of Pisa
Pisa, Italy
vincenzo.lottici@unipi.it

Antonio Colicelli
Dept. Information Engineering
University of Pisa
Pisa, Italy
antonio.colicelli@unipi.it

Attilio Vaccaro *MBI srl*
Pisa, Italy
avaccaro@mbigroup.it

Francesca Caparrini
Institute for the BioEconomy (IBE)
Italian National Research Council
Florence, Italy
caparrini@lamma.toscana.it

Nicola Davini *MBI srl*
Pisa, Italy
ndavini@mbigroup.it

Ottavio M. Picchi
MBI srl
Pisa, Italy
opicchi@mbigroup.it

Giovanni Serafino *MBI srl*
Pisa, Italy
gserafino@mbigroup.it

Andrea Antonini
Institute for the BioEconomy (IBE)
Italian National Research Council
Florence, Italy
antonini@lamma.toscana.it

Alessandro Mazza
Institute for the BioEconomy (IBE)
Italian National Research Council
Florence, Italy
mazza@lamma.toscana.it

Samantha Melani
Institute for the BioEconomy (IBE)
Italian National Research Council
Florence, Italy
melani@lamma.toscana.it

Alberto Ortolani
Institute for the BioEconomy (IBE)
Italian National Research Council
Florence, Italy
ortolani@lamma.toscana.it

Elisa Adirosi
Inst. Atmospheric Sciences and Climate
Italian National Research Council
Rome, Italy
elisa.adirosi@artov.isac.cnr.it

Luca Baldini
Inst. Atmospheric Sciences and Climate
Italian National Research Council
Rome, Italy
l.baldini@isac.cnr.it

Giovanni Rallo
Dept. Agriculture, Food and Environment
University of Pisa
Pisa, Italy
giovanni.rallo@unipi.it

Frederick S. Policelli
Goddard Space Flight Center Natl. Aeron. Space Admin. (NASA)
Greenbelt, MD, United States
frederick.s.policelli@nasa.gov

George J. Huffman
Goddard Space Flight Center Natl. Aeron. Space Admin. (NASA)
Greenbelt, MD, United States
george.j.huffman@nasa.gov

***Abstract*—This paper presents a practical application of an opportunistic technique for the estimation of rainfall intensity and accumulated precipitation. The proposed technique is based upon signal strength measurements made by commercial-grade interactive satellite terminals. By applying some processing, the rain-induced attenuation on the microwave downlink from the satellite is first evaluated; then the rain attenuation is eventually mapped into a rainfall rate estimate via a tropospheric model. This methodology has been applied to a test area of 30×30 km^2 around the city of Dortmund (North Rhine-Westphalia, upper basin of Ermscher river), for the heavy rain event that devastated western Germany in July, 2021. A rainfall map on this area is obtained from the measurements collected by a set of satellite terminals deployed in the region, and successfully compared with a map obtained with a conventional weather radar.**

***Keywords*—Rainfall rate estimation, satellite-to-ground links, signal of opportunity, rain fading**

I. Introduction

Quantitative precipitation estimation can be obtained by several observing systems using different measurement principles that have different time and space resolutions, and accuracies [1]. For instance, rain gauges (RGs) are point devices which can measure the accumulated rainfall (in mm) in a given amount of time and at a given location. Thus, maps of the cumulated rainfall can be obtained by resorting to networks of RGs, which are, however, usually characterized by a spatially inhomogeneous density. Disdrometers are other point-measurement instruments, but are still considered research devices and are less common than RGs. Concerning remote sensing devices, satellite sensors, though available on a global scale, suffer from scarce time and space resolution, whereas weather radars have a higher temporal (from 5 to 10 minutes) and spatial resolution (less than 1 km, although not uniform). Note also that there are regions of the globe where networks of sensing devices (in some cases, including RGs) are not available.

In the last few decades, the opportunistic use of pre-existing microwave (μW) communication links has been investigated to retrieve precipitation estimates. The basic idea is to estimate rainfall intensity relying on the attenuation due to the presence of precipitation along the propagation path, which affects either terrestrial links (e.g., backhaul connections in cellular networks), or the downlink of direct-to-home (DTH) satellite broadcasting, at Ku-band (10-13 GHz). In particular, satellite-based opportunistic systems for rain monitoring [2], powered by dedicated algorithms [3], [4], turn out to be very appealing due to: *i*) the wide diffusion over the territory already-installed DTH satellite receivers which can, in principle, act as rain sensing devices, prospectively allowing for a considerable geographical capillarity, at least in densely populated areas; *ii*) the ease of installation of new terminals to obtain higher spatial density; and *iii*) the low cost of commercial-grade satellite receive equipment.

Opportunistic measurements of μW satellite downlink, suitably pre-processed via an ensemble Kalman filter (EnKF) methodology [5], have been used in [6] to improve the measurements from a sparse RG network in the Düsseldorf area and enabled a more detailed spatio-temporal reconstruction of the rainfall fields for the catastrophic event that devastated western Germany in July 2021.

In this paper, with reference to the same location and event as in [6], we show how an already-operational network of DTH terminals could be used, as a standalone system, to provide accurate estimation of the accumulated rainfall and for rainfall map retrieval, at no additional cost.

The remainder of the paper is organized as follows. Sect. II describes the satellite platform and terminal characteristics. Sect. III illustrates the strategy for rainfall estimation based upon satellite signal measurements, including the tropospheric model. Sect. IV presents some numerical results and, finally, in Sect. V some conclusions are drawn and future perspectives for this research outlined.

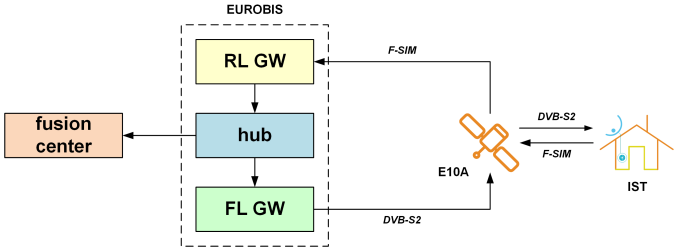

Fig. 1. Architecture of the EUROBIS platform.

Fig. 2. IoT FIRST two-way terminal: 80-cm satellite dish and IST [7].

II. Satellite platform

A. Platform architecture and terminals

The opportunistic measurements used in this case study are made by a population of interactive satellite systems (ISTs) and collected via satellite by a remote fusion center, taking advantage of an interactive satellite-based platform.

More in detail, the satellite infrastructure is offered by the EUROBIS IoT FIRST platform, a bidirectional, satellite-based interactive system owned and operated by Eutelsat S.A. The EUROBIS platform, operating in Ku band and linear polarization using Eutelsat 10A satellite in 10° E orbital position, provides an IP-based, transparent communication between a population (in the order of thousands units) of ISTs, called IoT FIRST terminals, and the Internet.

A high-level architecture of the EUROBIS platform is illustrated in Fig. 1, in which the hub controls both a forward-link (FL) gateway (GW) and a return-link (RL) GW. The FL makes use of a satellite link using digital video broadcasting satellite - version 2 (DVB-S2) [8]. The RL GW makes use of the enhanced spread-spectrum Aloha (E-SSA) protocol, in the version standardized by the European telecommunications standards institute (ETSI) as fixed satellite interactive multimedia (F-SIM) [9], [10]. The E-SSA-based RL adapts consolidated solutions from terrestrial cellular standards to the satellite scenario, using asynchronous access based on code division multiple access (CDMA) and iterative detection and interference cancellation to enable coexistence of a very large number of ISTs (up to millions). The main EUROBIS system parameters are summarized in Table I, which reports: *a*) the frequency and polarization of the downlink carrier employed for rain attenuation measurements by the ISTs;

Table I
EUTELSAT EUROBIS PLATFORM: MAIN PARAMETERS AND FEATURES OF FL AND RL.

parameter/feature	FL	RL
frequency [MHz]	11,345.8	14,216.6
polarization	vertical linear	horizontal linear
PHY protocol	DVB-S2	F-SIM
LL protocol	IP-MPE	F-SIM
EIRP [dBW]	48	–
G/T [dB/K]	–	+4
modcod format	QPSK 4/5	n/a

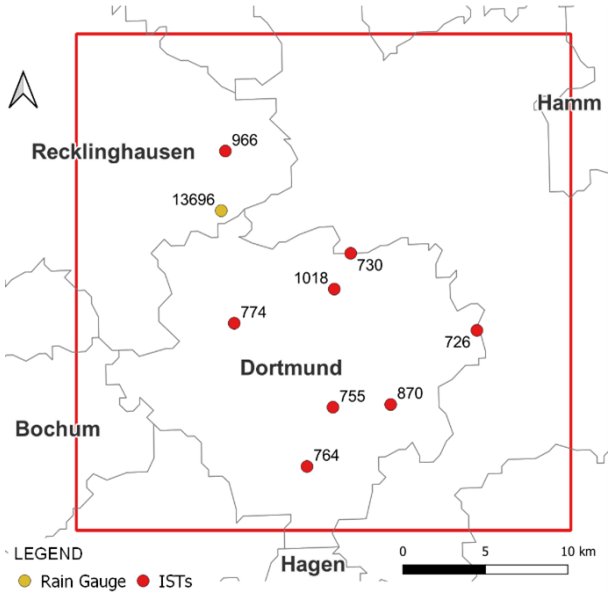

Fig. 3. Locations of rain sensing devices in the Dortmund area.

b) the physical-layer (PHY) and link-layer (LL) protocols, where MPE stands for multi-protocol encapsulation; and *c*) the transmission parameters, consisting of the effective isotropic radiated power (EIRP), the figure of merit G/T of the receive antenna, and the modulation and coding (modcod) format.

The ISTs used in this study are the so-called IoT FIRST terminals [11], a generation of very small aperture terminal (VSAT) low-cost, low-power satellite devices (depicted in Fig. 2), mainly used for internet of things (IoT) and machine-to-machine (M2M) applications. Each IST is able to measure the signal-to-noise ratio (SNR) in the FL using DVB-S2 parameters on a regular basis, and to send it to the fusion center via the EUROBIS platform through the RL.

B. Test area in Germany

The presence of several ISTs in the Nordrhein-Westfalen area, as shown in Fig. 3, enabled a detailed investigation of the extreme rain event which occurred on July 14-15, 2021. The study area considered in this paper is a square region of size 30×30 km^2 surrounding the city of Dortmund, Germany, whose vertex coordinates are indicated in Table II. Only one operational RGs of the German Deutscher

Table II
WGS84 COORDINATES OF THE VERTICES OF THE STUDY AREA.

vertex	longitude (° E)	latitude (° N)
NW	7.2743	51.6907
NE	7.7082	51.6963
SW	7.2844	51.4211
SE	7.7158	51.4266

Table III
WGS84 COORDINATES OF THE RAIN SENSING DEVICES.

device ID	longitude (° E)	latitude (° N)
RG 13696	7.4048	51.5966
IST 726	7.6306	51.5344
IST 730	7.5189	51.5749
IST 755	7.5061	51.4911
IST 764	7.4845	51.4586
IST 774	7.4183	51.5356
IST 870	7.5565	51.4932
IST 966	7.4073	51.6290
IST 1018	7.5052	51.5553

Wetterdienst (DWD) weather service [12] is accessible for the area (see Fig. 3), so the availability of additional opportunistic measurements from the ISTs can be very useful to accurately retrieve a localized precipitative phenomenon. For the reader's convenience, RGs and IST coordinates are listed in Table III.

Note that the DWD network consists of approximately 1,100 RGs [12] across Germany, whose surface is approximately 360,000 km^2. Then, the average density results of one device every 327 km^2 (i.e., 18×18 km^2). Instead, in the test area we have 8 ISTs, yielding a density of one device every 112.5 km^2 (i.e., 10.6×10.6 km^2).

III. OPPORTUNISTIC RAINFALL ESTIMATION FROM SATELLITE SIGNAL STRENGTH MEASUREMENTS

From a merely conceptual standpoint, the opportunistic rain sensing method adopted in this study is based on measurements of μW link attenuation and exploits the popular power law [2]

$$A/L = \gamma = \alpha \cdot R^{\beta}, \tag{1}$$

where A [dB] represents the total additional attenuation experienced by the signal strength level during the rain ("wet" condition) with respect to (wrt) the pre-rain value ("dry" condition), L [km] is the length of the "wet" radio path, γ [dB/km] is the relevant specific attenuation, R [mm/h] is the rain rate (assumed constant along the path L), and α and β are frequency- and polarization-dependent empirical coefficients.

The value of L to be put in (1) can be derived from simple considerations about the link geometry. To this respect, Fig. 4 shows the geometry of a slanted satellite "wet" link through the rain, assuming the simpler tropospheric model [13]. The satellite elevation θ over the horizon is a known design parameter: e.g., for the reception in Dortmund, Germany (lat.

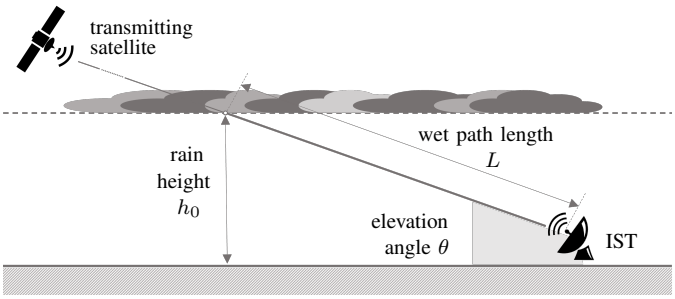

Fig. 4. Geometry of a slanted satellite "wet" link through rain.

7.4684295° E, lon. 51.514244° N) of Eutelsat 10A satellite (lon. 10° E), the elevation turns out to be 31°. The rain height h_0 can be derived from the knowledge of the 0°C isotherm height provided by a short-term forecast based on weather models (WRF, MOLOCH, BOLAM, etc.) or can be a fixed value based on daily or yearly averages taken at the receive location.

The value of the attenuation A to be put in (1) can be evaluated from the measurements of the signal strength or the SNR η, which is directly provided by the receiving device itself. Most commercial receivers for satellite broadcasting provide a measurement of the ratio $\eta = E_s/N_0$ between the energy per symbol E_s and the one-sided power spectral density of the noise N_0, so that the attenuation can be obtained as [4]

$$A = \frac{\eta^{\mathsf{dry}}}{\eta^{\mathsf{rain}}}\,(1-\xi)+\xi, \tag{2}$$

where the superscript dry denotes the reference level for the evaluation of the rain attenuation (suitably pre-stored during clear sky days), while rain denotes the current reading during the precipitation, and ξ is a design parameter which depends on the noise contributions affecting the received signal (see [4, eq. (4)]).

It is worth remarking that accurate rain sensing actually requires suitably adapted relationships, still derived from (1), which account for the more complex and layered structure of the troposphere (e.g., including the melting layer) [4].

IV. Numerical results

We analyze, for each IST located according to the coordinates introduced in Sect. II, the samples collected starting from 05:50 UTC, on July 14, 2021. The estimated isothermal height during this event has been 4 km. As an example of such measurements, Fig. 5 depicts the data collected by IST 966. The blue line reports the measurements of $\eta = E_s/N_0$, whereas the red line corresponds to the estimated rain rate obtained by processing the records using algorithm described in [4], and sketched in Sect. III.

Based on this data set, we are able to provide an estimate of the cumulated rain, as depicted in Fig. 6 for each IST in the selected region. The measures provided by the RG 13696 are also reported using the dashed black curve. The results for IST 966, which is the closest one to the RG and whose

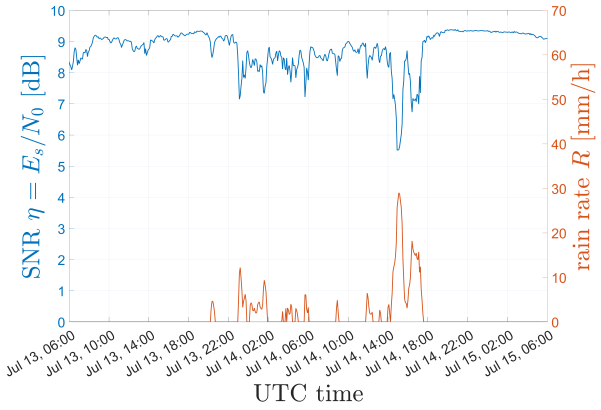

Fig. 5. Sample records of $\eta = E_s/N_0$ measured from the IST 966 (in blue) and estimates of the rain rate (in red).

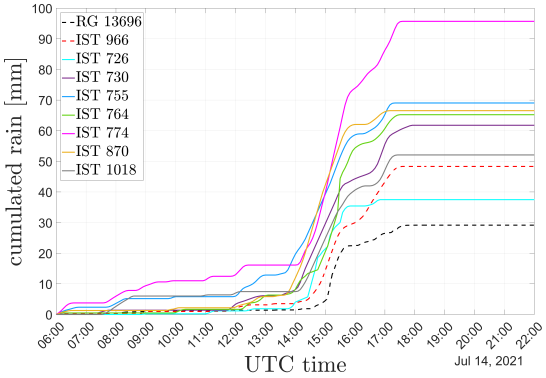

Fig. 6. Cumulated rain provided by the ISTs and the RG 13696 in the Dortmund area (July 14, 2021).

instantaneous results can be observed in Fig. 5, are reported using the dashed red line.

In order to retrieve the rain event within the area of interest, a spatialization technique is applied to the cumulated rain recorded by rain sensing devices. The study area is divided into 100×100 squares, each with size 300×300 m^2. The interpolation method used is the inverse distance weighting (IDW) interpolation, which assumes that the assigned values to unknown points are calculated with a weighted average of the values available at the known points, according to

$$r\,(k) = \left(\sum_{n=1}^{N} \frac{r_n}{d_{n,k}^4}\right) \Bigg/ \left(\sum_{n=1}^{N} \frac{1}{d_{n,k}^4}\right), \tag{3}$$

where N is the number of the rain sensing devices, r_n are the cumulated rain values measured by device n, and $d_{n,k}$ is the distance from device n to the kth square. This means that values closer to known points have a bigger weight compared to farther values.

By applying (3) to the measurements obtained by the ISTs and the RG, we obtain the rainfall map reported in Fig. 7. This can be compared to that produced by a weather radar [14], and reported in Fig. 8 for the reader's convenience.

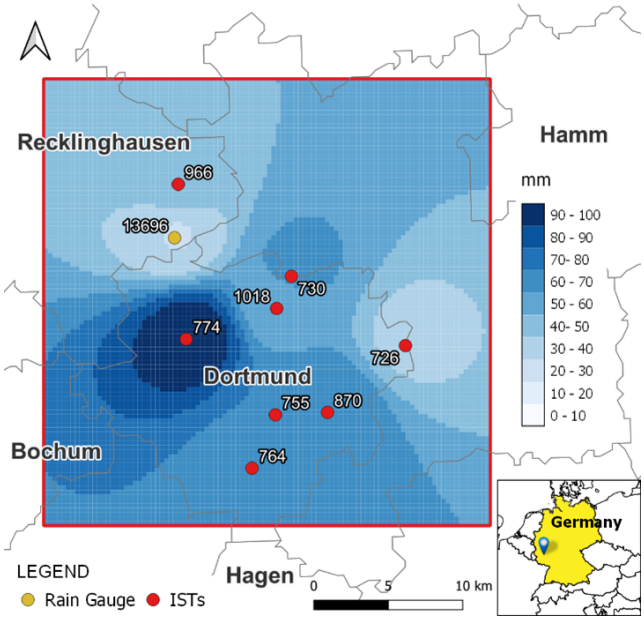

Fig. 7. Cumulated rain on the test area from July 14, 2021 05:50 UTC, to July 15, 2021 05:50 UTC, obtained from the signal attenuation measured by the network of ISTs plus the measurements of one RG.

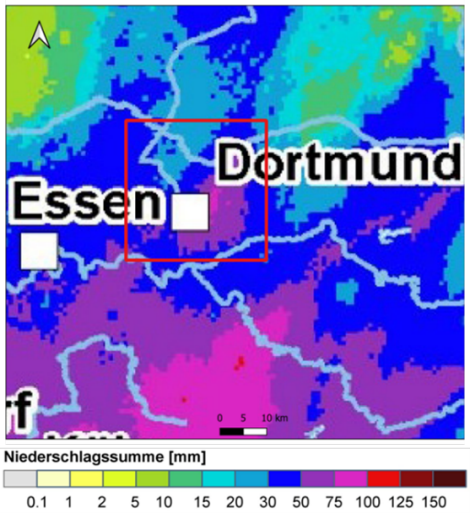

Fig. 8. Cumulated rain on the test area (square box) from July 14, 2021 05:50 UTC, to July 15, 2021 05:50 UTC, obtained from a weather radar [14].

First, it is interesting to note that the RG id:13696, reported in Fig. 3 and whose measurements are shown in Fig. 6, is located marginally wrt the area affected by the most intense precipitation, as can be deduced from the radar map in Fig. 8. This is the reason why, in Fig. 6, the RG provides a cumulated rain value which is lower than those of the IST-based sensors.

Second, note that there is just one available RG in an area of 900 km^2 and, even worse, in this specific case study it seriously underestimates the rain event under observation. This fact dramatically highlights the limits of a pluviometric network made only of conventional RGs.

Finally, as apparent by comparing the rainfall maps of Figs. 7 and 8, the retrieval technique based on the opportunistic use of the ISTs yields the following benefits:

- *high accuracy*: the numerical estimates of the cumulated rain are in good agreement with weather radar measurements;
- *high reliability*: the spatial reconstruction of the precipitation field has a shape which is very similar to that detected by the weather radar;
- *high spatial resolution*: the retrieved map has a better resolution than the one provided by the weather radar (and, if needed, the resolution can be suitably scaled by deploying more terminals);
- *high temporal resolution*: the measurement of the satellite signal strength (and therefore the estimate of the rain rate, too) is typically provided at a rate of 1 or 2 readings per minute;
- *low cost*: only low-cost commercial-grade devices (already installed) were used and no installation of new equipment was required;
- *no electromagnetic emissions*: rain sensing is simply based on the reception of satellite broadcast signals.

V. Conclusions and Future Developments

The tests carried out for the extreme rain event in Germany demonstrated the feasibility and the potentials of a network of DTH satellite receive terminals for opportunistic rainfall estimation. These tests represent a preliminary phase of a broad experimental campaign to be carried out in the framework of the EU funded SCORE project [15], which aims to increase climate resilience in European coastal cities. The project is tackling specific c hallenges r elated t o s ea levels, coastal erosion and extreme weather events using an integrated solution of smart technologies and nature-based solutions to be developed and tested in ten selected European coastal cities. In the future, we also expect to investigate if and how similar data can be combined together and with satellite estimates of rainfall such as the NASA Imerg data [16] to produce improved precipitation monitoring over large areas.

Acknowledgment

This work was supported by the project INSIDERAIN (INStruments for Intelligent Detection and Estimation of Rain for Agricultural INnovation) [17], funded by Tuscany regional administration (Italy), Decreto n. 21885, 18/12/2020, and by the project SCORE (Smart Control of the Climate Resilience in European Coastal Cities) [15], funded by European Commission's Horizon 2020 research and innovation programme under grant agreement no. 101003534. This article is also based upon work from COST Action CA20136 OPENSENSE, supported by COST (European Cooperation in Science and Technology).

REFERENCES

[1] E. Adirosi, L. Facheris, F. Giannetti, S. Scarfone, G. Bacci, A. Mazza, A. Ortolani, , and L. Baldini, "Evaluation of rainfall estimation derived from commercial interactive DVB receivers using disdrometer, rain gauge, and weather radar," *IEEE Trans. Geosci. Remote Sens.*, vol. 59, no. 11, pp. 8978–8991, Nov. 2021.

[2] F. Giannetti and R. Reggiannini, "Opportunistic rain rate estimation from measurements of satellite downlink attenuation: A survey," *MDPI Sensors*, vol. 21, no. 17, p. 5872, Aug. 2021.

[3] F. Giannetti, R. Reggiannini, M. Moretti, E. Adirosi, L. Baldini, L. Facheris, A. Antonini, S. Melani, G. Bacci, A. Petrolino, and A. Vaccaro, "Opportunistic rain rate estimation from measurements of satellite downlink attenuation: A survey," *MDPI Sensors*, vol. 17, no. 8, p. 1864, Aug. 2017.

[4] F. Giannetti, M. Moretti, R. Reggiannini, and A. Vaccaro, "The NEFOCAST system for detection and estimation of rainfall fields by the opportunistic use of broadcast satellite signals," *IEEE Aerospace and Electronic Systems Mag.*, vol. 34, no. 6, pp. 16–27, Jun. 2019.

[5] A. Ortolani, F. Caparrini, S. Melani, L. Baldini, and F. Giannetti, "An EnKF-based method to produce rainfall maps from simulated satellite-to-ground MW-link signal attenuation," *J. Hydrometeorology*, vol. 22, no. 5, pp. 1333–1350, May 2021.

[6] A. Ortolani, F. Caparrini, S. Melani, A. Antonini, A. Mazza, F. Giannetti, F. Sapienza, L. Facheris, L. Baldini, E. Adirosi, and A. Vaccaro, "An EnKF-based reconstruction of rainfall fields using opportunistic satellite MW link signal attenuation: Theoretical basis and application to the July 2021 event in the area of Dortmund (Germany)," in *Living Planet Symposium*, Bonn, Germany, May 2022.

[7] Egatel S.L. (2022) IoT First terminal. [Online]. Available: https://www.egatel.es/producto/iot-first-terminal

[8] *Digital Video Broadcasting (DVB); Second generation framing structure, channel coding and modulation systems for Broadcasting, Interactive Services, News Gathering and other broadband satellite applications; Part 1: DVB-S2*, Std. ETSI EN 302 307-1 V1.4.1, Nov. 2014.

[9] Eutelsat, DLR, and MBI, "Air interface for fixed satellite interactive multimedia (F-SIM): Link layer and system signalling specification," Tech. Rep. Draft 2.0, 2017.

[10] Eutelsat, "Satellite earth stations and systems; air interface for fixed satellite interactive multimedia (F-SIM); part 3: Physical layer specification, return link asynchronous access," Tech. Rep. v. 1.01.04, 2013.

[11] Eutelsat S.A. (2022) IoT services. [Online]. Available: https://www.eutelsat.com/en/satellite-communication-services/satellite-iot-connectivity.html

[12] T. Winterrath, W. Rosenow, and E. Weigl, "On the DWD quantitative precipitation analysis and nowcasting system for real-time application in german flood risk management," in *Proc. Intl. Symp. Weather Radar and Hydrology*, Exeter, UK, Apr. 2011.

[13] International Telecommunication Union (ITU) - R, "Rain height model for prediction methods," ITU-R, Geneva, Switzerland, Tech. Rep. Recommendation P.839-4, 2013.

[14] Deutscher Wetterdienst. (2022) Wetter und Klima aus einer Hand. [Online]. Available: https://www-cdn.eumetsat.int/files/2021-07/Precip Analysis DWD floodArea.jpg

[15] Smart control of the climate resilience in European coastal cities (SCORE). (2022) Project website. [Online]. Available: https://score-eu-project.eu

[16] G. J. Huffman, "NASA Global Precipitation Measurement (GPM) Integrated Multi-Satellite Retrievals for GPM (IMERG)," NASA, Tech. Rep. NASA Algorithm Theoretical Basis Doc. version 06, Mar. 2019.

[17] INStruments for Intelligent Detection and Estimation of Rain for Agricultural INnovation (INSIDERAIN). (2022) Project website. [Online]. Available: https://www.insiderain.it/